Structural Engineering and Mechanics, *Vol. 59, No. 5 (2016) 803-820*
DOI: http://dx.doi.org/10.12989/sem.2016.59.5.803

Evaluation of a DDB design method for bridges isolated with triple pendulum bearings

Gholamreza Ghodrati Amiri[*1], Mahdi Mohammadian Shalmaee[2a] and Pejman Namiranian[3b]

[1]*Center of Excellence for Fundamental Studies in Structural Engineering, School of Civil Engineering, Iran University of Science and Technology, Tehran, Iran*
[2]*Department of Civil Engineering, Faculty of Engineering, University of Guilan, Rasht, Iran*
[3]*School of Civil Engineering, Iran University of Science and Technology, Tehran, Iran*

(Received December 28, 2015, Revised March 2, 2016, Accepted April 4, 2016)

Abstract. In this study a direct displacement-based design (DDBD) procedure for a continuous deck bridge isolated with triple friction pendulum bearings (TFPB) has been proposed and the seismic demands of the bridge such as isolator's displacement and drift of piers obtained from this procedure evaluated under two-directional near-field ground motions. The structural model used here are continuous, three-span, cast-in-place concrete box girder bridge with a 30-degree skew which are isolated with 9 different TFPBs. By comparing the results of DDBD method with those of nonlinear time history analysis (NTHA), it can be concluded that the proposed procedure is able to predict seismic demands of similar isolated bridges with acceptable accuracy. Results of NTHA shows that dispersion of peak resultant responses for a group of ground motions increases by increasing their average value of responses. It needs to be noted that the demands parameters calculated by the DDBD procedure are almost overestimated for stiffer soil condition, but there is some underestimation in results of this method for softer soil condition.

Keywords: direct displacement-based design; triple friction pendulum bearing; seismic isolation; bridge; near field ground motion

1. Introduction

Seismic isolation is a response modification technique used to protect structures from potential damages caused by strong ground motions. Isolation uncouples a structure from potential earthquake damages by increasing the flexibility of the system beyond the predominant periods of ground excitations along with providing an appropriate damping ratio. These modifications can be applied to a structure by installing a mechanical device named isolator, usually in the base of structure (or between pier and deck in bridge cases), Therefore, an isolator should have not only adequate flexibility to lengthen the vibration period of the system in order to reduce the design

∗Corresponding author, Professor, E-mail: Ghodrati@iust.ac.ir
[a]Ph.D. Student
[b]Ph.D.

http://www.techno-press.org/?journal=sem&subpage=8 ISSN: 1225-4568 (Print), 1598-6217 (Online)

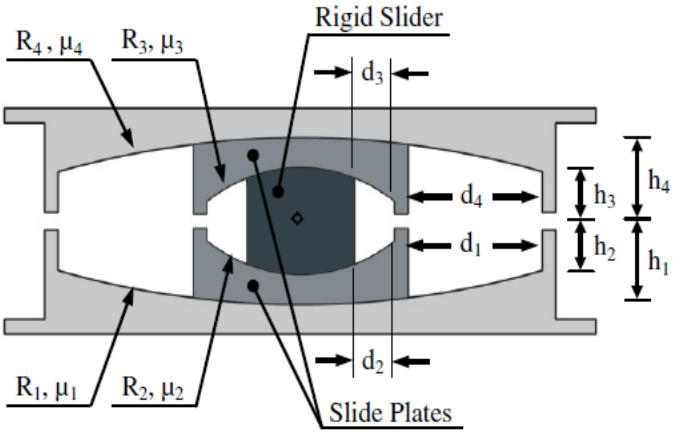

Fig. 1 Geometric and friction parameters of a TFPB (Amiri and Namiranian 2014)

forces, but also an energy dissipation mechanism to increase the damping ratio of the system to an appropriate level. Furthermore it should show enough rigidity when subjected to service loads.

There are various types of isolators introduced in literature and even used in practical cases. Triple Friction Pendulum Bearings (TFPBs) which is classified as sliding isolators, recently developed by Fenz and Constantinou (2008b), In sliding isolators, the friction between sliders implemented as the factor of energy dissipation and the act of sliding cause the flexibility of the system. As shown in Fig. 1 a TFPB includes multiple concave surfaces that depending on the level of displacement, sliding occurs between various surfaces. Regarding the fact that the lateral stiffness of a sliding isolator varies with characteristics change of its sliding surfaces (i.e., friction coefficient and radius of curvature), the force-displacement response of a TFPB would be multi stage and multi linear as illustrated in Fig. 2. In spite of some advantages of this adaptive behavior, it makes it difficult to model and analyze TFPBs for design purposes in comparison to other simpler isolators.

Codes and specifications for isolation systems such as TFPBs provide two types of analysis procedure for calculating the seismic demands (i.e., the isolator displacement and base shear force) of structures: simplified methods and nonlinear time history analysis (NTHA), The latter can be cumbersome to use, specially when this situation comes together with complicity of TFPBs. Recently some studies conducted to model TFPBs in nonlinear time history analysis (Fenz and Constantinou 2008a, Yurdakul and Ates 2011), Simplified methods have therefore been developed such that the entire structural system (including superstructures, substructures and isolation systems) is modeled as a single degree of freedom (SDOF) system with an equivalent effective stiffness and an equivalent viscous damping ratio to represent the energy dissipation. The effective stiffness of an isolation system ($K_{e,is}$) can easily be calculated by knowing the force transmitted to isolator (F) and the displacement of isolator (D_{is}), as formulated in Eq. (1)

$$K_{e,is} = \frac{F}{D_{is}} \tag{1}$$

The equivalent viscous damping ratio of an isolation system ($\xi_{eq,is}$) is calculated based on the well-known Jacobsen's equation (Chopra 1995)

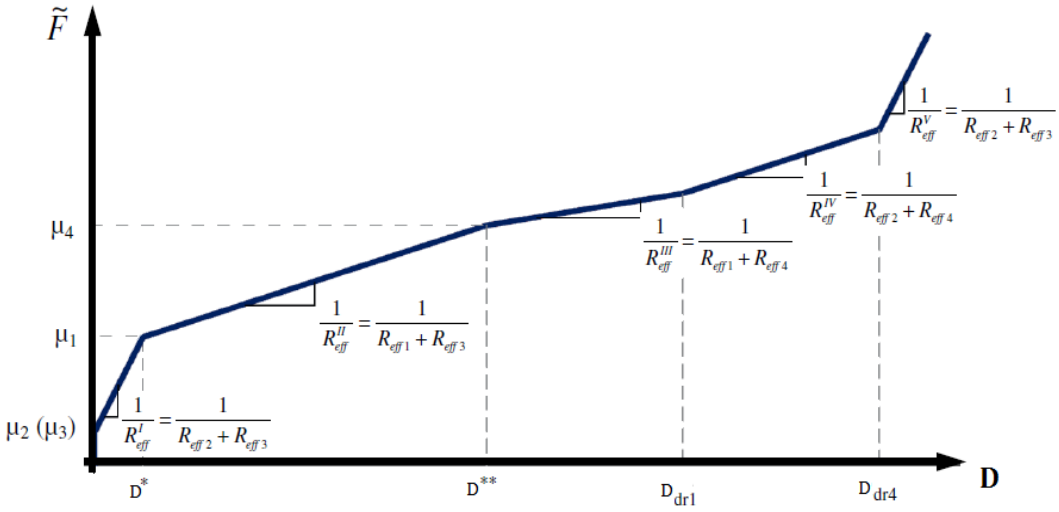

Fig. 2 Normalized force-displacement relationship for a TFPB (Amiri and Namiranian 2014)

$$\xi_{eq,is} = \frac{Hysteretic\ Energy\ Dissipated}{2\pi K_{e,is} D_{is}^{2}} \tag{2}$$

In Eq. (2), which is suitable for displacement dependent isolators such as TFPBs, Hysteretic Energy Dissipated is the total energy dissipated by the isolator in the cycle of maximum amplitude and is equal to the area under the hysteresis curve of the isolator. With determination of the effective stiffness and the equivalent viscous damping ratio of the isolation system those of entire structural system can be developed. So the seismic demands can be calculated from a design spectrum by applying damping modification factor.

Direct Displacement-Based Design (DDBD) is a displacement-based simplified method proposed by Priestley (1993), new displacement-based methods, such as DDBD, are more compatible with performance-based concepts of earthquake engineering in comparison with traditional force-based ones, because performance levels are described in terms of displacements. The fundamental goal of DDBD is to obtain a structure which will reach a target displacement profile when subjected to earthquakes consistent with a given reference response spectrum.

In recent years many studies have been published about evaluating accuracy of simplified methods in seismic designing and analyzing of different kind of structures (Sullivan *et al*. 2014, Jara and Casas 2006, Kowalsky 2002), Fadi and Constantinou (2010) evaluated the accuracy of simplified methods in analyzing structures that are supported on TFPBs under one-directional far-field ground motions. Amiri and Namiranian (2014) evaluated the accuracy of capacity spectrum method (CSM), which is a simplified method, in estimating seismic demands of TFPBs under near-field ground motions. They concluded that CSM can provide a good estimation for isolator displacements and base shear forces.

An early displacement-based approach for the design of bridges with seismic isolation can be found in Priestley *et al*. (1996), Calvi and Pavese (1997), Recently Priestley *et al*. (2007) proposed the extension of the DDBD method to bridges with seismic isolation. Calvi *et al*. (2008) presented a review of displacement-based seismic design of structures, including seismically isolated

bridges. Cardone *et al*. (2009) proposed a DDBD algorithm for seismically isolated bridges with various types of isolators. Tecchio *et al*. (2015) and Mergos (2013) examined the accuracy of DDBD on RC bridge bents.

This study aimed to propose a Direct Displacement-Based Design (DDBD) method for a seismically isolated bridge with Triple Friction Pendulum Bearings (TFPBs) and then to evaluate it's accuracy under two-directional near-field ground motions. Results of current paper may confirm reliability of simplified methods in analyzing and designing of seismically isolated structures with triple friction pendulum bearings.

2. A DDBD for isolated bridges

2.1 The step-by-step procedure of DDBD for a isolated bridge

Following assumptions should be considered in implementation of DDBD for isolated bridges (Buckle *et al*. 2006): (1) The bridge superstructure acts as a diaphragm that is rigid in-plane and flexible out-of- plane. Compared to the flexibility of the isolators, bridge superstructures are relatively rigid and this assumption is applicable to a wide range of superstructure types. (2) For cases which are relatively simple in plan and elevation the bridge may be modeled as a single-degree-of-freedom system. (3) The displacement response spectrum for the bridge site is linearly proportional to period within the period range of the isolated bridge (i.e., the spectral velocity is constant and the spectral acceleration is inversely proportional to the period in this range), (4) Hysteretic energy dissipation can be represented by equivalent viscous damping. (5) The design response spectrum may be scaled for different viscous damping ratios by damping factors which are independent of period.

The DDBD for isolated bridges can be performed in four general steps. In the first step the target displacement profile (Δ_i) is set by the designer such that the desired performance level could be achieved for a given seismic hazard level. For bridge cases, codes and specifications provides limited values of deck's displacement and pier's drift for a given performance level. The design displacement can be developed using the following equation (Priestley 2003)

$$\Delta_d = \frac{\sum_{i=1}^{n}\left(m_i \,.\, \Delta_i^2\right)}{\sum_{i=1}^{n}\left(m_i \,.\, \Delta_i\right)} \tag{3}$$

Where n is the number of piers and abutments, m_i is the appropriate contribution of deck (and pier) mass at each abutment (or pier) location and Δ_i is the corresponding deck displacement. Regarding the first assumption mentioned above (that the superstructure of bridge is rigid) the corresponding deck displacement at each pier (or abutment) location would be the same and then equal to the design displacement, as the superstructures of the bridge models are continuous.

In the second step, the nonlinear MDOF model of the bridge is replaced by an equivalent linear SDOF system, whose properties (K_e and β_{eq}) correspond to the effective lateral stiffness and equivalent viscous damping of the real bridge at the peak displacement response. The effective lateral stiffness of the equivalent SDOF system would be the sum of equivalent stiffness of all pier (or abutment)-isolator systems

$$K_e = \sum_{i=1}^{n} K_i \tag{4}$$

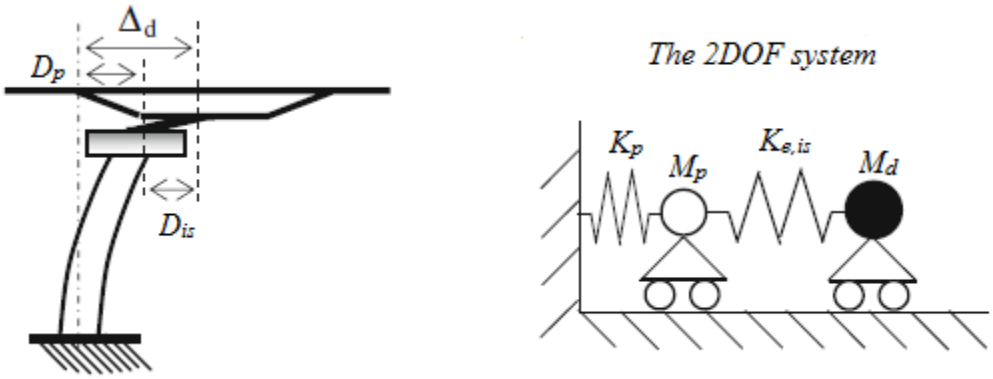

(a) Distribution of design displacement in piers (b) The 2DOF model of pier-isolators-deck system

Fig. 3 A pier-isolator-deck system

Where n is the number of piers and abutments and K_i is the equivalent stiffness of ith pier (or abutment)-isolator system. As the abutments assumed to be rigid, K_i at abutment locations is equal to effective lateral stiffness of isolation system. K_i at pier locations can be calculated from following equation

$$\frac{1}{K_i} = \frac{1}{K_p} + \frac{1}{2K_{e,is}} \tag{5}$$

Where K_p is the elastic stiffness of the pier, and $K_{e,is}$ is the effective lateral stiffness of each isolator. So for calculation of K_i, either at abutment or pier location, it is necessary to determine the effective lateral stiffness of isolators. On the other hand as illustrated in Eq. (1), $K_{e,is}$ is a function of isolator's displacement which is unknown. Fig. 3 shows the distribution of the design displacement between pier and isolators (which is $\Delta_d=D_{is}+D_p$) and the corresponding 2DOF model. From this relationship and analyzing The 2DOF system through a trial and error procedure, the isolator's displacement can be obtained at pier locations. But at abutment locations the design displacement is fully allocated to the isolators, as the abutments assumed to be rigid.

The equivalent viscous damping ratio of the SDOF system can be obtained from below

$$\beta_{eq} = \frac{\sum_{i=1}^{n}(m_i \,.\, \beta_{eq,i})}{\sum_{i=1}^{n}(m_i)} \tag{6}$$

Where n is the number of piers and abutments, m_i is the appropriate contribution of deck (and pier) mass at each pier (or abutment) location and $\beta_{eq,i}$ is the equivalent viscous damping ratio of ith pier (or abutment)-isolator system. $\beta_{eq,i}$ at abutment locations is same as the equivalent viscous damping ratio of isolators (ξ_{is}) and at pier locations can be calculated from following equation

$$\beta_{eq,i} = \frac{D_{p,i} \,.\, \xi_{p,i} + D_{is,i} \,.\, \xi_{is,i}}{D_{p,i} + D_{is,i}} \tag{7}$$

Where $D_{p,i}$ and $\xi_{p,i}$ are the corresponding pier's displacement and damping ratio, and $D_{is,i}$ and $\xi_{is,i}$ are the corresponding isolator's displacement and equivalent viscous damping ratio respectively. The damping ratio of both models without seismic isolation assumed to be 2% and

Table 1 Geometric Configuration of TFPBs used in bridges models

Designation	Displacement Capacities (mm)			Effective Radius (mm)	
	d_2=d_3	d_1=d_4	$d_{Tot.}$	R_{eff2}=R_{eff3}	R_{eff1}=R_{eff4}
GC1	64	228	584	356	1499
GC2	125	400	1050	300	2085
GC3	178	356	1524	902	3823

Table 2 Friction coefficient values of surfaces used in bridge models

Designation	Surface 1		Surface 2		Surface 3		Surface 4	
	μ_{max}	μ_{min}	μ_{max}	μ_{min}	μ_{max}	μ_{min}	μ_{max}	μ_{min}
LF	0.04	0.02	0.02	0.01	0.02	0.01	0.1	0.05
HF	0.07	0.04	0.02	0.01	0.02	0.01	0.14	0.07
EF	0.07	0.04	0.02	0.01	0.02	0.01	0.07	0.04

the equivalent viscous damping ratio of isolators can be calculated from Eq. (2),

Once the elastic properties of the equivalent SDOF system is developed, in the third step the effective period of vibration (T_e) associated with the design displacement can be determined from the following well-known equation

$$T_e = 2\pi\sqrt{\frac{m_e}{K_e}} \tag{8}$$

Where m_e is the effective mass of the equivalent SDOF system and equals to the mass of the deck plus mass of the upper one-third of piers. It needs to be noted that if the design displacements at pier and abutment locations (Δ_i) aren't identical, then the effective mass can be expressed as a function of Δ_i (Priestley *et al.* 2003)

$$m_e = \frac{\sum_{i=1}^{n} m_i \Delta_i}{\Delta_d} \tag{9}$$

Since the effective period of the equivalent SDOF system is determined, the displacement of the SDOF system (D_d) can be obtained from a displacement response spectrum which is modified to the equivalent viscous damping ratio (β_{eq}) level by applying a damping modification factor.

In the fourth step the displacement obtained from previous step (D_d) is compared with the design displacement (Δ_d) which is defined in the first step. If $|D_d - \Delta_d| < \varepsilon$,then the results are acceptable and other parameters such as base shear forces can be calculated, else someone may go back to the first step and change the initial design parameters such as configuration of isolators, size of sections and even the design displacements, and repeat the procedure until convergence is achieved. The base shear force at piers is equal to the pier's drift (D_p) multiple in it's stiffness (K_p).

2.2 Description of the isolated bridge model

A bridge model isolated with 9 different TFPBs has been considered. Table 1 shows the geometric configuration of isolators (effective radius and displacement capacity) and Table 2 shows three different sets of friction coefficients (low friction, high friction and equal friction)

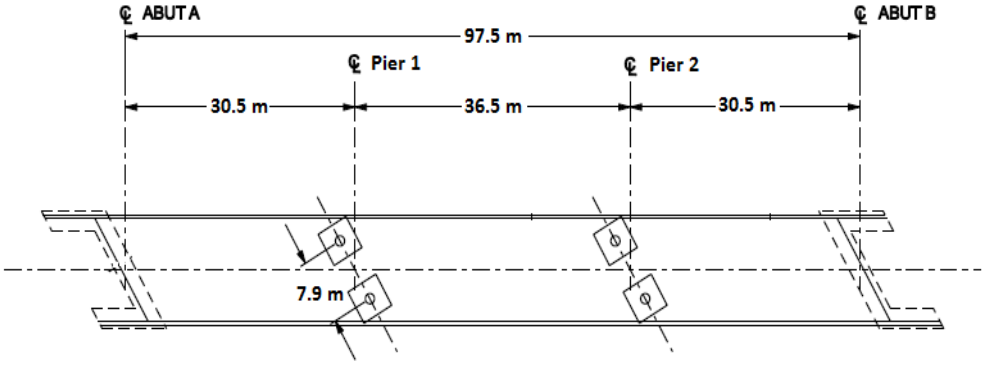

Fig. 4 Plan view of the bridge model with same height of piers equal to 6 meter

used for each of these geometrical configurations, Where μ_{max} is the coefficient of friction at high velocity and μ_{min} is the coefficient of friction at very slow velocity. In Table 2 the values of μ_{max} and μ_{min} have been obtained from results of experimental tests conducted by previous studies (Fenz and Constantinou 2008c, Mokha *et al*. 1993), These isolators were used before in some previous studies (Amiri and Namiranian 2014, Fadi and Constantinou 2010).

The structural model is a continuous, three-span, cast-in-place concrete box girder bridge with a 30-degree skew. The bridge was used as an example of bridge design without an isolation system in the Federal Highway Administration Seismic Design Course, Design Example No. 4 (document available through NTIS, document no. PB97-142111),

Fig. 4 shows the bridge model described above. This model is the modified form of the design example for seismic isolation application. It has three traffic lanes and isolated with two isolators at each abutment and pier location. Loadings were determined based on AASHTO LRFD Specifications with live load consisting of truck, lane and tandem and wind load being representative of typical sites in the Western United States. Loading results show that the total weight (the critical combination of live and dead loads) supported by each isolator at the abutment and pier locations is approximately equal to 2350 kN and 5750 kN, respectively.

Each pier consists of two circular columns which are connected by a rigid beam as a cap, so the pier works as a frame in the direction of rigid beam and as a cantilever in the direction normal to the beam. By setting the direction normal to the deck as *x* direction and the direction of the deck as *y* direction, and regarding the 30 degrees skew of the bridge, the stiffness of each pier is calculated from below

$$K_{px} = \frac{1}{\sqrt{\frac{cos30^2}{\left(\frac{24EI}{L^3}\right)^2} + \frac{sin30^2}{\left(\frac{6EI}{L^3}\right)^2}}} \tag{10}$$

$$K_{py} = \frac{1}{\sqrt{\frac{sin30^2}{\left(\frac{24EI}{L^3}\right)^2} + \frac{cos30^2}{\left(\frac{6EI}{L^3}\right)^2}}} \tag{11}$$

Table 3 Parameters of the series model of a TFPB for the most general configuration

SFBP	Coefficients of friction	Effective radius of curvature	Nominal displacement capacities	Rate parameter
Element 1	$\bar{\mu}_1 = \mu_2 = \mu_3$	$\bar{R}_{eff1} = R_{eff2} + R_{eff3}$	$\bar{d}_1 = (d_1 + d_2 + d_3 + d_4) + (\bar{d}_2 + \bar{d}_3)$	$\bar{a}_1 = \frac{(a_2 + a_3)}{4}$
Element 2	$\bar{\mu}_2 = \mu_1$	$\bar{R}_{eff2} = R_{eff1} - R_{eff2}$	$\bar{d}_2 = \frac{R_{eff1} - R_{eff2}}{R_{eff1}} d_1$	$\bar{a}_2 = \frac{R_{eff1}}{R_{eff1} - R_{eff2}} a_1$
Element 3	$\bar{\mu}_3 = \mu_4$	$\bar{R}_{eff3} = R_{eff4} + R_{eff3}$	$\bar{d}_3 = \frac{R_{eff4} - R_{eff3}}{R_{eff4}} d_4$	$\bar{a}_3 = \frac{R_{eff4}}{R_{eff4} - R_{eff3}} a_4$

Where *E*, *I* and *L* are the elasticity modulus of concrete, the moment of inertia of each circular section and columns' length respectively. It needs to be noted that all foundations of both models assumed to be rigid in this study.

3. Nonlinear Time History Analysis (NTHA)

3.1 Equation of motion

The complicated hysteretic behavior of TFPBs makes it difficult to model them in the analysis and design methods specially in the time history analysis. But the hysteretic behavior of the TFPBs can be simulated by a series model of three independent Single Friction Pendulum Bearing (SFPB) elements, as shown in Fig. 5. Each element of the series model, which is connected to other elements with a slider mass, consists of a parallel arrangement of a linear elastic spring element representing the restoring force provided by the curvature of the spherical dish ($1/\bar{R}_{effi}$), a rigid plastic friction element with velocity dependence ($\bar{\mu}_i$) and a gap element to account for the finite displacement capacity of each sliding surface ($\bar{d}_i$), The characteristics of each element of the series model are defined such that the hysterical behavior of the series model as a whole matches to the corresponding real TFPB. The defined parameters are summarized in Table 3 (Fenz and Constantinou 2008b),

Considering a tow-directional analysis for a orthogonal directions of *x* and *y*, the force produced by the described arrangement of each element is given by (Fenz and Constantinou 2008)

$$F_{ix} = \frac{W}{\bar{R}_{effi}} u_{ix} + \bar{\mu}_i W Z_{ix} + K_{ri}\left(|u_i| - \bar{d}_i\right) sign(u_i) H\left(|u_i| - \bar{d}_i\right).\frac{u_{ix}}{u_i} \tag{12}$$

$$F_{iy} = \frac{W}{\bar{R}_{effi}} u_{iy} + \bar{\mu}_i W Z_{iy} + K_{ri}\left(|u_i| - \bar{d}_i\right) sign(u_i) H\left(|u_i| - \bar{d}_i\right).\frac{u_{iy}}{u_i} \tag{13}$$

Where *W* is the weight supported by each isolator, u_{ix} and u_{iy} are the relative displacement of *i*th SFPB element of the series model in the *x* and *y* directions, u_i is the radial relative displacement of *i*th SFPB element of the series model ($u_i = ({u_{ix}}^2 + {u_{iy}}^2)$^0.5), K_{ri} is the stiffness after gap closing, which should be assigned a large value, and H denotes the Heaviside function. Z_{ix} and Z_{iy} are dimensionless hysteretic variables of *i*th SFPB element. These are

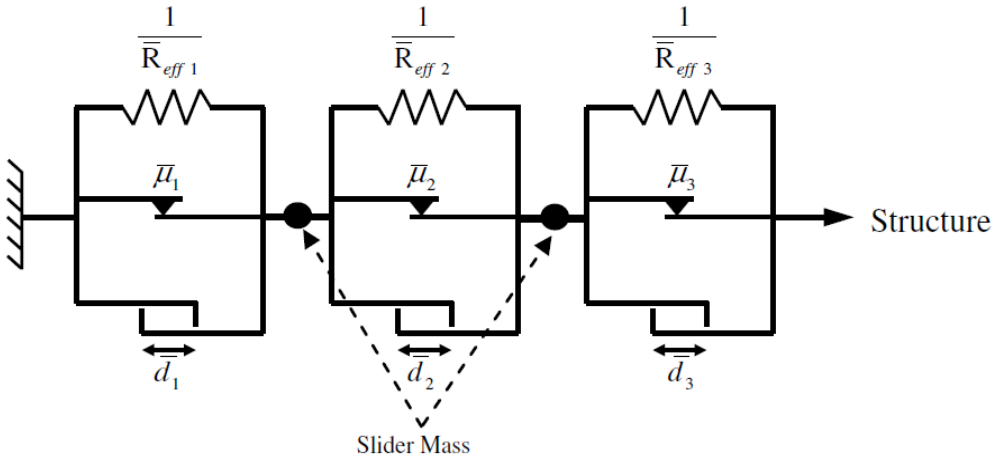

Fig. 5 The series model of three SFPBs for modeling a TFPB

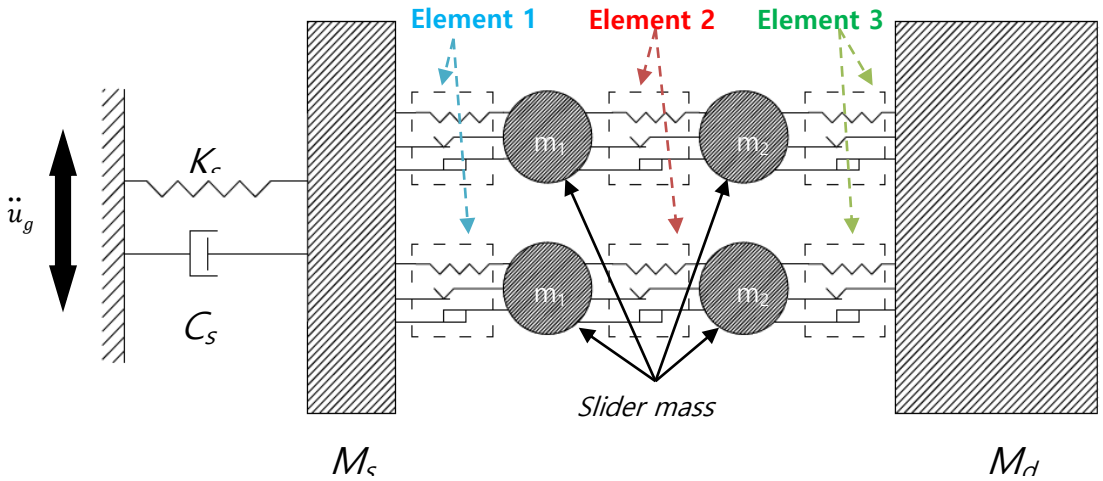

Fig. 6 mathematical model of a substructure-TFPBs-deck system for the bridge model

essentially the equations that are used for dynamic analysis of FP bearings (Nagarajaiah 1991), The only difference is the last term of equations, which is the additional restoring force from contacting the displacement restrainer.

The coefficient of friction at each sliding interface ($\bar{\mu}_i$) varies with velocity according to the following equation

$$\bar{\mu}_i = \mu_{max} - (\mu_{max} - \mu_{min})e^{-a|\dot{u}_i|} \tag{14}$$

Where μ_{max} is the coefficient of friction at high velocity, μ_{min} is the coefficient of friction at very slow velocity, a is a rate parameter, which has units of time per unit length and controls the variation between μ_{max} and μ_{min}, and $\dot{u}_i$ is the relative sliding velocity of ith SFPB element of the series model.

Fig. 6 shows the mathematical model of a substructure-TFPBs-deck system for the bridge model. Assuming a same displacement in all along the deck, The dynamic behavior of such a system subjected to a ground motion can be described by the following eight degrees of freedom: u_{dx} and u_{dy} are the displacement of the deck, u_{sx} and u_{sy} are the displacement of substructure, and u_{1x}, u_{1y}, u_{2x}, u_{2y} are the displacements of the slider masses. The effect of vertical excitation is ignored, because according to experimental studies, it does not have any significant effects on the prediction of the responses of a structure supported by the TFPBs (Fenz and Constantinou 2008a, Morgan 2007), So the motion equations of the system subjected to a ground motion in the *x* directions can be given by

$$\begin{bmatrix} m_d & 0 & 0 & 0 \\ 0 & m_2 & 0 & 0 \\ 0 & 0 & m_1 & 0 \\ 0 & 0 & 0 & m_s \end{bmatrix} \begin{Bmatrix} \ddot{u}_{dx} \\ \ddot{u}_{2x} \\ \ddot{u}_{1x} \\ \ddot{u}_{sx} \end{Bmatrix} + \begin{bmatrix} 0 & 0 & 0 & 0 \\ 0 & 0 & 0 & 0 \\ 0 & 0 & 0 & 0 \\ 0 & 0 & 0 & C_{Sx} \end{bmatrix} \begin{Bmatrix} \dot{u}_{dx} \\ \dot{u}_{2x} \\ \dot{u}_{1x} \\ \dot{u}_{sx} \end{Bmatrix} + \begin{bmatrix} 0 & 0 & 0 & 0 \\ 0 & 0 & 0 & 0 \\ 0 & 0 & 0 & 0 \\ 0 & 0 & 0 & K_{Sx} \end{bmatrix} \begin{Bmatrix} u_{dx} \\ u_{2x} \\ u_{1x} \\ u_{sx} \end{Bmatrix}$$
$$= -\begin{bmatrix} m_d & 0 & 0 & 0 \\ 0 & m_2 & 0 & 0 \\ 0 & 0 & m_1 & 0 \\ 0 & 0 & 0 & m_s \end{bmatrix} \begin{bmatrix} 1 & 0 & 0 & 0 \\ 0 & 1 & 0 & 0 \\ 0 & 0 & 1 & 0 \\ 0 & 0 & 0 & 1 \end{bmatrix} \ddot{u}_{gx} - 2 \begin{Bmatrix} F_{3x} \\ F_{2x} - F_{3x} \\ F_{1x} - F_{2x} \\ -F_{1x} \end{Bmatrix} \quad (15)$$

Where m_1 and m_2 are the masses, very small, assigned to the slider, m_d is the appropriate contribution of deck mass, m_s is the mass of substructure which is assumed to be zero in abutments and one-third of pier mass in pier locations, K_{Sx} and C_{Sx} are the stiffness and damping coefficient of the substructure. A relatively large value assigned to K_{Sx} in abutments in order to model the rigidity of abutments. $\ddot{u}_{gx}$ is the horizontal component of ground motions in the *x* direction and F_{ix} is the force in the *i*th isolator element. Similarly, the equation of motion in the *y* direction can be written as the *x* direction.

Since the Z_i variables change very slowly when the bearing is sliding and change very rapidly in the regions where the direction of motion reverses or when sticking occurs, the governing equations are systems of stiff differential equations (Fenz and Constantinou 2008a), So in order to solve the equations correctly, first, the time step in the solution algorithm should have a very small value (0.005 sec has been found suitable), and second, a special algorithm for solving these types of equations should be implemented (Shampine and Reichelt 1997), The equations of motion of the substructure-TFPBs-deck system can be expressed as a system of first-order ordinary differential equations as below

$$\{\dot{x}\} = [A]\{x\} + \{B\} \quad (16)$$

Where the state vector $\{x\}$ is

$$\{x\} = \{u_{sx}\ u_{sy}\ \ u_{1x}\ u_{1y}\ \ u_{2x}\ u_{2y}\ \ u_{dx}\ u_{dy}\ \ u_{sx}\ \ u_{sy}\ \ u_{1x}\ \ u_{1y}$$
$$u_{2x}\ \ u_{2y}\ u_{dx}\ u_{dy}\ \ Z_{1x}\ Z_{1y}\ \ Z_{2x}\ \ Z_{2y}\ Z_{3x}\ Z_{3y}\}^T \quad (17)$$

The entries of matrix [*A*] and vector $\{B\}$ can be calculated from Eqs. (15), (16), (17) and the similar entries between vector $\{x\}$ and vector $\{\dot{x}\}$ (first to eighth entries of $\{\dot{x}\}$ is equal to ninth to sixteenth entries of $\{x\}$), These 22 first-order ordinary differential equations are solved simultaneously by using the *ode15s* solver in MATLAB. The *ode15s* solver is a variable order, multi-step algorithm that is appropriate for solving systems of stiff differential equations.

Table 4 Characteristics of near-field ground motions for SR soil condition

Earthquake	Station	Magnitude (M_w)	Distance (km)	Component	PGA (g)	PGV (cm/s)	PGD (cm)
Chi Chi (CC057)	TCU057	7.6	11.8	Normal	0.12	34.5	55.3
				Parallel	0.09	41.0	57.0
Cape Mendocino (CMP)	Petrolia	7	8.2	Normal	0.61	81.9	25.5
				Parallel	0.63	60.4	26.0
Duzce (DB)[a]	Bolu	7.1	12	Normal	0.79	54.8	22.7
				Parallel	0.78	62.5	13.5
Gazli (GK)	Karakyr	6.8	5.5	Normal	0.60	64.9	24.2
				Parallel	0.71	71.1	24.7
Kokaeli (KG)[a]	Gebze	7.5	10.9	Normal	0.24	52.0	44.1
				Parallel	0.14	28.2	25.4
Kokaeli (KI)	Izmit	7.5	7.2	Normal	0.15	22.6	9.8
				Parallel	0.22	29.8	17.1
Northridge (NN)[a]	Newhall	6.7	5.9	Normal	0.72	120.1	35.1
				Parallel	0.65	49.9	16.2
Northridge (NR)[a]	Rinaldi	6.7	6.5	Normal	0.87	167.1	28.8
				Parallel	0.42	62.6	21.4
Northridge (NS)[a]	Sylmar	6.7	5.3	Normal	0.59	130.3	54.0
				Parallel	0.80	93.3	53.3
Tabas (TT)	Tabas	7.4	2	Normal	0.81	118.3	96.8
				Parallel	0.81	79.6	42.1

[a] Pulse subset records

3.1 Ground motions and scaling methods

Near-field ground motions may be distinguished from far field ones by some characteristics such as distinctive pulse-like time histories, high peak velocities, and large ground displacements. Previous studies show that seismically isolated structures are sensitive to near-field ground motions such that their response are qualitatively different when subjected to these kind of ground motions. Near-field ground motions, especially pulse-like records, may cause an extra displacement demand to isolated systems and need more attention for selecting the locations and properties of isolators.

Twenty pairs of near-field ground motions in two sets, one for stiff Soil to soft Rock (SR) condition and another for soft Soil to stiff Soil (SS) condition, are used to evaluate the accuracy of the DDBD method in estimating the seismic demand parameters of isolated bridges with TFPBs. These ground motions are used previously to evaluate the accuracy of equivalent lateral force procedure in estimating seismic displacement of lead rubber bearings (Ozdemir and Constantinou 2010) and also to evaluate the accuracy of capacity spectrum method in estimating seismic demands of TFPBs (Amiri and Namiranian 2014), Tables 4 and 5 show the main characteristics of these motions, which were downloaded from PEER Strong Motion Database. Among these records

Table 5 Characteristics of near-field ground motions for SS soil condition

Earthquake	Station	Magnitude (M_w)	Distance (km)	Component	PGA (g)	PGV (cm/s)	PGD (cm)
Chi Chi (CC101)[a]	TCU101	7.6	2.1	Normal	0.22	68.4	71.9
				Parallel	0.24	53.0	41.6
Erzincan (EE)[a]	Erzincan	6.7	4.4	Normal	0.49	95.4	32.1
				Parallel	0.42	45.3	16.5
Imperial Valley (IVA4)[a]	El Centro Array#4	6.5	7	Normal	0.36	77.9	58.7
				Parallel	0.47	40.1	20.7
Imperial Valley (IVA5)[a]	El Centro Array#5	6.5	4	Normal	0.38	91.5	62.0
				Parallel	0.53	49.0	37.0
Imperial Valley (IVA6)[a]	El Centro Array#6	6.5	1.4	Normal	0.44	111.8	66.5
				Parallel	0.40	64.7	24.8
Imperial Valley (IVA10)[a]	El Centro Array#10	6.5	6.2	Normal	0.18	47.0	31.4
				Parallel	0.23	39.3	18.9
Kocaeli (KD)	Duzce	7.5	15.4	Normal	0.28	52.1	37.9
				Parallel	0.38	53.2	26.7
Kocaeli (KY)[a]	Yarimca	7.5	4.8	Normal	0.28	48.2	43.0
				Parallel	0.31	72.9	55.9
Loma Prieta (LPCor)	Corralitos	6.9	3.9	Normal	0.48	45.4	14.1
				Parallel	0.51	41.6	7.20
Loma Prieta (LPSar)[a]	Saratoga	6.9	8.5	Normal	0.36	55.5	29.4
				Parallel	0.38	43.3	15.8

[a] Pulse subset records

which are rotated to fault parallel and normal component, 14 records show the property of pulses (pulse subset) as judged by wavelet analysis classification of the records (Baker 2007), These time histories represent near-field ground motions from recorded historic events which have a variety of faulting mechanisms in the magnitude range of 6.5 to 7.6 and distance range of 1-16 km.

Scaling of ground motions is performed in two separate stages. In the first step, the geometric-mean scaling method presented by Huang (2008) is implemented to normalize the records. In this method the sum of the squared errors between the target spectral values and the scaled geometric mean of the spectral ordinates for each pair is minimized in some specified periods (1,2,3,4 and 5 s based on Ozdemir and Constantinou (2010)), Table 6 shows the scaling factors for each record obtained by using geometric-mean scaling method and ASCE7-10 spectra as target spectral values.

The second stage of scaling is performed according to the ASCE requirements. For each pair of horizontal ground motion components, a SRSS (Square Root of the Sum of Squares) spectrum shall be constructed by taking the SRSS of the 5%-damped response spectra for the scaled components (where an identical scale factor is applied to both components of each pair), The ASCE requires that each pair of ground motions shall be scaled such that in the period range from $0.5T_D$ to $1.25T_M$, the average of the SRSS spectra from all horizontal component pairs does not fall below the corresponding ordinate of the design spectrum used for the site, where T_D and T_M are

Table 6 Scale factors of geometric-mean scaling method

SR soil condition			SS soil condition		
Ground motion	Scale factor		Ground motion	Scale factor	
	DBE	MCE		DBE	MCE
CC057	1.33	1.99	CC101	1.68	2.53
CMP	0.68	1.02	EE	0.97	1.46
DB	0.6	0.9	IVA4	1.26	1.89
GK	0.81	1.22	IVA5	1.05	1.58
KG	1.58	2.37	IVA6	0.88	1.32
KI	1.67	2.5	IVA10	1.91	2.86
NN	0.7	1.05	KD	1.22	1.83
NR	0.54	0.81	KY	0.96	1.44
NS	0.41	0.62	LPCor	1.49	2.24
TT	0.56	0.84	LPSar	1.67	2.51

Table 7 Equivalent viscous damping ratio of TFPBs in different conditions

Isolator's configuration - friction condition	β_{eq} (%)			
	SR soil condition		SS soil condition	
	DBE	MCE	DBE	MCE
GC1-LF	20	11.6	17.7	14
GC1-HF	19.3	20.6	20.8	15.1
GC1-EF	26.1	19.6	21	15
GC2-LF	22.3	20.7	21.8	16.5
GC2-HF	23.6	24	27.1	22.4
GC2-EF	32	25.1	26.7	18.7
GC3-LF	21.4	20.7	20.7	18.8
GC3-HF	24	20	21	20.9
GC3-EF	30.2	27.7	28.7	27.2

defined as the effective periods in the DBE and MCE hazard levels. Because of the different configuration and surface properties of each isolator, T_D and T_M are different for each isolation system, so the second stage scaling factors will be different for each TFPB considered in this study. The final scaling factor for each near-field motion is obtained by multiplying the scaling factor derived from the two separate stages.

4. Analysis results

This study used ASCE7-10 spectra as the design spectra which are in two hazard levels (DBE and MCE) and for two soil types (stiff Soils to soft Rocks (SR) and soft Soils to stiff Soils (SS)), The proposed DDBD procedure is coded in MATLAB and is run for each described model (1 structural models with 9 different TFPBs) in two directions (normal to deck (x) and parallel to

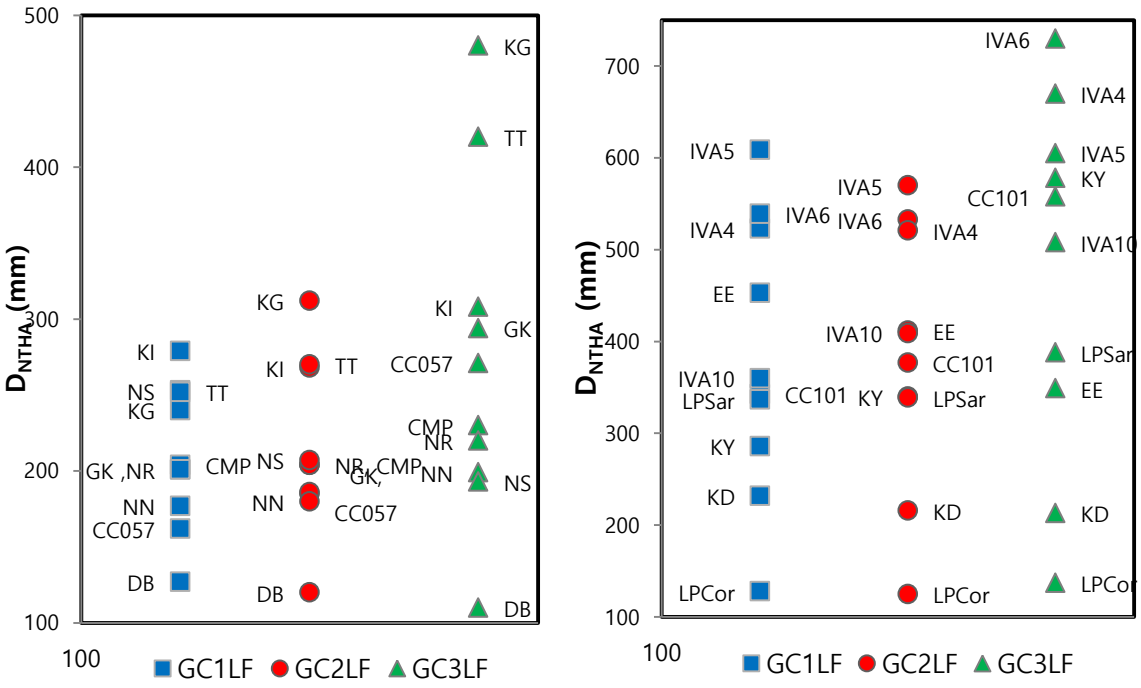

(a) SR soil condition (b) SS soil condition

Fig. 7 dispersion of isolator's peak resultant response obtained from each pair of time histories for DBE hazard level

deck (y)) and for the mentioned ASCE7-10 design spectra. For each case, the results of DDBD method is evaluated by the corresponding results obtained from Nonlinear Time History Analysis (NTHA),

The isolation systems have an effective period, T_{eff}, in the range of 2.3-3.9 and 2.6-4.4 s in the DBE and MCE hazard levels respectively, and an equivalent viscous damping ratio, β_{eq}, in the range of 18-32% and 12-27% of critical in the DBE and MCE hazard levels, respectively. The detailed values of β_{eq} presented in Table 7.

Fig. 7 shows dispersion of isolator's peak resultant response $\left(\sqrt{u_y^2 + u_x^2}\right)$ obtained from each pair of time histories for the SR and SS ground motion groups. It can be seen that dispersion of peak resultant responses for a ground motion group increases by increasing their average value of responses.

Fig. 8 shows a comparison of the peak isolator displacement at piers calculated by the proposed DDBD method based on the orthogonal combination rule $\left(\sqrt{u_y^2 + 0.3u_x^2}\right)$ and the average value of the maximum resultant displacement $\left(\sqrt{u_y^2 + u_x^2}\right)$ calculated by NTHA for the SR and SS soil condition in two seismic hazard levels. Maximum difference between the DDBD and the average of NTHA is about 8% and 11%, respectively, for DBE and MCE hazard levels in the case of SR soil condition, and the majority of results are overestimated by the proposed method. The maximum difference in the case of SS soil condition is raised to 9% and 8% for DBE and MCE hazard levels, respectively and some results are underestimated by the proposed method.

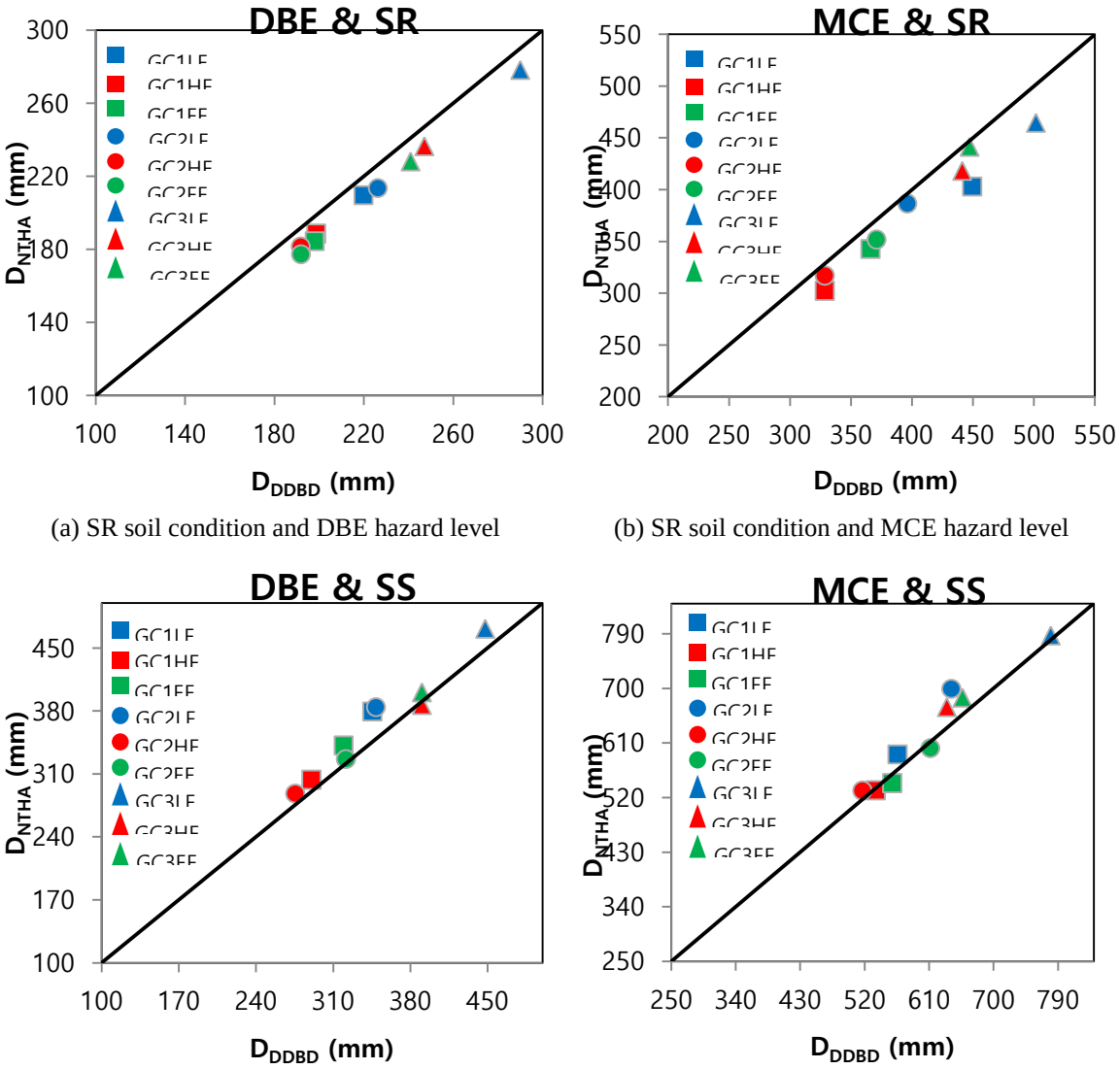

(a) SR soil condition and DBE hazard level

(b) SR soil condition and MCE hazard level

(c) SS soil condition and DBE hazard level

(d) SS soil condition and MCE hazard level

Fig. 8 Comparison of NTHA and DDBD on TFPB displacements in different conditions

Pier's drift, which is directly related to the base shear forces of the bridge models, is another parameter of interest for evaluation of the proposed DDBD results in this study. For the case of SR soil condition, maximum difference of pier's drift between the DDBD results and the average of NTHA is about 9% and 8% for DBE and MCE hazard levels, respectively. The maximum difference in the case of SS soil condition is about 10% and 11% for DBE and MCE hazard levels, respectively and almost all results are overestimated by the proposed method. Fig. 9 shows the corresponding results of both methods of analysis for pier's drift.

The results of this study demonstrate that the proposed DDBD method is able to predict the

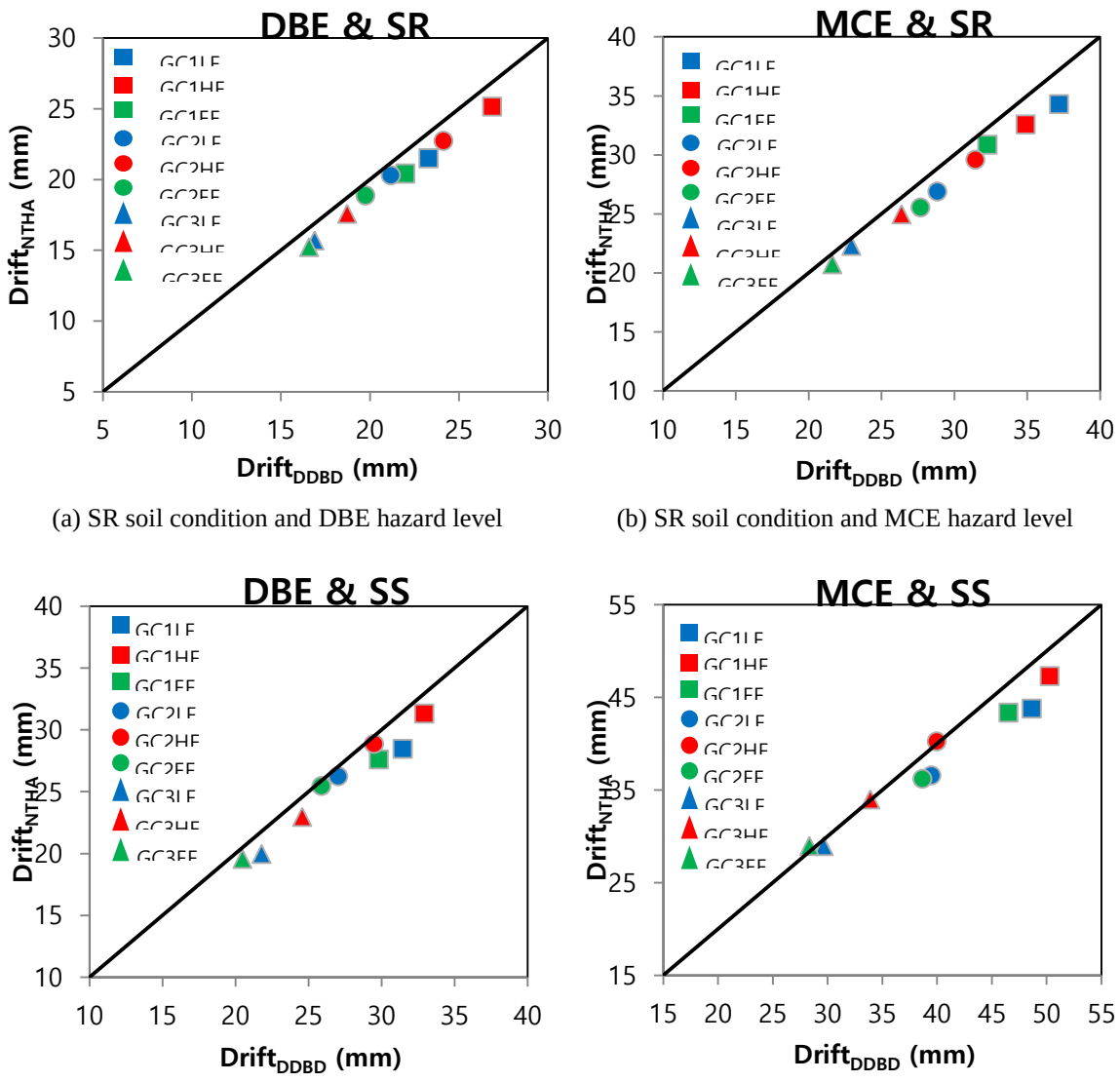

(a) SR soil condition and DBE hazard level

(b) SR soil condition and MCE hazard level

(c) SS soil condition and DBE hazard level

(d) SS soil condition and MCE hazard level

Fig. 9 Comparison of NTHA and DDBD on drift of piers in different conditions

seismic demands of bridges supported on TFPBs with acceptable accuracy. This conclusion is generally in agreement with the results of previous studies on the simplified methods for different isolation systems and seismic excitations. However, it should be noted that for the case of softer soil condition, there is some underestimation in the calculated seismic demands by the DDBD procedure, this gives the reason that codes and standards should not allow the usage of these methods without the aid of a NTHA.

5. Conclusions

The DDBD method is one of the displacement-based simplified procedures for calculating the seismic demands of isolated structures under ground motions. In this study, comparisons have been made between the DDBD results and those of NTHA under near-field excitations for a continuous, three-span, cast-in-place concrete box girder bridge isolated with TFPBs.

Because of the complicated hysteretic behavior of TFPBs, a series model of three SFPBs implemented for modeling them in nonlinear time history analysis. Results of NTHA shows that dispersion of peak resultant responses for a ground motion group increases by increasing their average value of responses.

Generally, results of both methods show that TFPBs with bigger configuration and lower friction coefficients have more displacement demand but cause less drift of pier, on the other hand TFPBs with smaller configuration and bigger friction coefficients have less displacement demand but cause more drift of pier. Therefore, depending on the design limitations such as available clearance and dimension of sections, an appropriate configuration and friction coefficients could be selected.

Based on the comparison of the isolator displacements and drift of piers for the two approaches, it is concluded that the proposed DDBD method can predict these seismic demands in a good agreement with the mean of the results by the NTHA. But for the soft soil (SS) condition, some results are underestimated by the DDBD, compared with those of the NTHA. In spite of simplicity and acceptable result of the DDBD, it is not error-free. Simplified methods such as DDBD can be used for preliminary design purposes and for checking the results of NTHA.

References

AASHTO LRFD (2005), *bridge design specifications*, American Association of State Highway and Transportation Officials, USA

Amiri, G.G. and Namiranian, P. (2014), "Evaluation of capacity spectrum method in estimating seismic demands of triple pendulum bearings under near-field ground motions", *Int. J. Struct. Stab. Dyn.*, **14**(2), 1350062.

ASCE (2010), *Minimum design loads for buildings and other structures*, American Society of Civil Engineering, USA.

Baker, J.W. (2007), "Quantitative classification of near-fault ground motions using wavelet analysis", *Bull. Seismol. Soc. Am.*, **97**(5), 1486-1501.

Buckle, I.G., Constantinou, M.C., Diceli, M. and Ghasemi, H. (2006), "Seismic isolation of highway bridges", MCEER, USA.

Calvi, G., Priestley, M. and Kowalsky, M. (2008), "Displacement-based seismic design of structures", *Paper presented at the 3rd National Conference on Earthquake Engineering and Engineering Seismology*.

Calvi, G.M. and Pavese, A. (1997), "Conceptual design of isolation systems for bridge structures", *J. Earthq. Eng.*, **1**(1), 193-218.

Cardone, D., Dolce, M. and Palermo, G. (2009), "Direct displacement-based design of seismically isolated bridges", *Bull. Earthq. Eng.*, **7**(2), 391-410.

Chopra, A.K. (1995), *Dynamics of Structures: Theory and Applications to Earthquake Engineering*, Prentice Hall, USA.

Fadi, F. and Constantinou, M.C. (2010), "Evaluation of simplified methods of analysis for structures with triple friction pendulum isolators", *Earthq. Eng.Struct. Dyn.*, **39**(1), 5-22.

Fenz, D.M. (2008), "Development, implementation and verification of dynamic analysis models for multi-

spherical sliding bearings", PhD Dissertation, State University of New York, Buffalo.
Fenz, D.M. and Constantinou, M.C. (2008a), "Modeling triple friction pendulum bearings for response-history analysis", *Earthq. Spectra*, **24**(4), 1011-1028.
Fenz, D.M. and Constantinou, M.C. (2008b), "Spherical sliding isolation bearings with adaptive behavior: Theory", *Earthq. Eng.Struct. Dyn.*, **37**(2), 163-183.
Fenz, D.M. and Constantinou, M.C. (2008c), "Spherical sliding isolation bearings with adaptive behavior: Experimental verification", *Earthq. Eng.Struct. Dyn.*, **37**, 185-205.
Huang, Y.N. (2008), "Performance assessment of conventional and base-isolated nuclear power plants for earthquake and blast loadings", PhD Dissertation, State University of New York, Buffalo.
Jara, M. and Casas, J.R. (2006), "A direct displacement-based method for the seismic design of bridges on bi-linear isolation devices", *Eng. Struct.*, **28**(6), 869-879.
Kowalsky, M.J. (2002), "A displacement-based approach for the seismic design of continuous concrete bridges", *Earthq. Eng.Struct. Dyn.*, **31**(3), 719-747.
Mergos, P.E. (2013) "The anchorage-slip effect on direct displacement-based design of R/C bridge piers for limiting material strains", *Comput. Concrete*, **11**(**6**), 493-513.
Mokha, A., Constantinou, M. and Reinhorn, A. (1993), "Verification of friction model of teflon bearings under triaxial load", *J. Struct. Eng.*, **119**(1), 240-261.
Morgan, T.A. (2007), "The use of innovative base isolation systems to achieve complex seismic performance objectives", PhD Dissertion, University of California, Berkeley.
Nagarajaiah, S., Reinhorn, A.M. and Constantinou, M.C. (1991), "3D-BASIS-nonlinear dynamic analysis of three-dimensional base isolated structures: Part II", Technical Report MCEER, New York, USA.
Ozdemir, G. and Constantinou, M.C. (2010), "Evaluation of equivalent lateral force procedure in estimating seismic isolator displacements", *Soil Dyn. Earthq. Eng.*, **30**(10), 1036-1042.
Priestley, J.N., Earthquake, S.O. and Dynamics, C.E. (2003), *Myths and fallacies in earthquake engineering, revisited*, IUSS Press, USA.
Priestley, M., Calvi, G. and Kowalsky, M. (2007), "Direct displacement-based seismic design of structures", *Paper presented at the 5th New Zealand Society for Earthquake Engineering Conference.*
Priestley, M.J.N. (1993), *Myths and fallacies in earthquake engineering: conflicts between design and reality*, IUSS Press, USA.
Priestley, M.N. (1996), *Seismic design and retrofit of bridges*, John Wiley & Sons, USA.
Shampine, L.F.and Reichelt, M.W. (1997), "The matlab ode suite", *SIAM J. Scientif. Comput.*, **18**(1), 1-22.
Sullivan, T., Welch, D. and Calvi, G. (2014), "Simplified seismic performance assessment and implications for seismic design", *Earthq. Eng. Eng. Vib.*, **13**(1), 95-122.
Tecchio, G., Marco, D. and Claudio, M. (2015), "Direct displacement-based design accuracy prediction for single-column RC bridge bents", *Earthq. Struct.*, **9**(3), 455-480.
Yurdakul, M. and Ates, S. (2011) "Modeling of triple concave friction pendulum bearings for seismic isolation of buildings", *Struct. Eng. Mech.*, **40**(3), 315-334.

CC